J Membrane Biol (2010) 234:171–181
DOI 10.1007/s00232-010-9244-7

Channel-Forming Abilities of Spontaneously Occurring α-Toxin Fragments from *Staphylococcus aureus*

Beatrix Vécsey-Semjén · Young-Keun Kwak · Martin Högbom · Roland Möllby

Received: 13 October 2009 / Accepted: 4 March 2010 / Published online: 26 March 2010

Abstract Pore formation by four spontaneously occurring α-toxin fragments from *Staphylococcus aureus* were investigated on liposome and erythrocyte membranes. All the isolated fragments bound to the different types of membranes and formed transmembrane channels in egg-phosphatidyl glycerol vesicles. Fragments of amino acids (aa) 9–293 (32 kD) and aa 13–293 (31 kD) formed heptamers, similar to the intact toxin, while the aa 72–293 (26 kD) fragment formed heptamers, octamers, and nonamers, as judged by gel electrophoresis of the liposomes. All isolated fragments induced release of chloride ions from large unilamellar vesicles. Channel formation was promoted by acidic pH and negatively charged lipid head groups. Also, the fragments' hemolytic activity was strongly decreased under neutral conditions but could be partially restored by acidification of the medium. We paid special attention to the 26-kD fragment, which, despite the loss of about one-fourth of the N-terminal part of α-toxin, did form transmembrane channels in liposomes. In light of the available data on channel formation by α-toxin, our results suggest that proteolytic degradation might be better tolerated than previously reported. Channel opening could be inhibited and open channels could be closed by zinc in the medium. Channel closure could be reversed by addition of EDTA. In contrast, digestion at the C terminus led to premature oligomerization and resulted in species with strongly diminished activity and dependent on protonation.

Keywords α-Toxin fragments · Hemolysis · Large unilamellar vesicles · Oligomerization · Channel formation

Y.-K. Kwak · R. Möllby
Department of Microbiology, Tumor and Cell Biology, Karolinska Institutet, 171 77 Stockholm, Sweden

B. Vécsey-Semjén (✉)
House of Science, Alba Nova University Centre, Royal Institute of Technology, 106 91 Stockholm, Sweden
e-mail: beatrix@vetenskapenshus.se

M. Högbom
Stockholm Center for Biomembrane Research, Department of Biochemistry and Biophysics, Arrhenius Laboratories for Natural Sciences, Stockholm University, 106 91 Stockholm, Sweden

Introduction

The biological relevance of α-toxin from *Staphylococcus aureus* was always coupled to the toxin's ability to form transmembrane channels and lyse target cells. In contrast to most bacterial pore-forming toxins, which need proteolytic activation for membrane insertion and channel formation to occur, α-toxin forms transmembrane channels without any further modification. α-Toxin is secreted by *S. aureus* as a water-soluble 33-kD monomer that binds to specific receptors, identified as sphingomyelin–cholesterol microdomains on rabbit erythrocytes (RRBC) (Hildebrand et al. 1991; Valeva et al. 2006). We still know but little about the membrane-bound monomer and the manner of oligomer formation. Recently Valeva et al. (2006) presented evidence that α-toxin binding to lipid microdomains clusters the monomers, and close proximity of the monomers leads to monomer–monomer binding and oligomer formation. In contrast, α-toxin attachment is thought to be transient on nonsensitive cell membranes and the same effect is achieved by high toxin concentrations. In this initial step of membrane binding, acidification of the medium might play a crucial role (Vecsey-Semjen et al. 1996). Also, here membrane binding orients the monomers so they can bind

to each other and form heptameric ring structures, presumably by lateral diffusion. We still do not know whether the membrane-bound monomers form a continuously growing chain until circularization or form smaller multimeric units that build oligomers by random encounters. In this stage the α-toxin oligomer is permanently anchored to the lipid membrane by an interaction(s) of a crevice in each monomer and the phosphocholine head groups in the membrane (Guillet et al. 2004; Vecsey-Semjen et al. 1997). Under favorable conditions oligomers go through conformational changes and insert into the lipid bilayer to form a homoheptameric channel. In the final transmembrane channel the N-terminal latch folds down into a cavity on the cap domain of the neighboring monomer (Song et al. 1996; Walker and Bayley 1995).

The cap domain harbors the main bulk of protein anchored to the lipid bilayer by the rim domain. The glycine-rich stem domain is connected to the cap domain by the triangle region. The stem domain inserts into the lipid bilayer and forms the antiparallel β-sheet that forms the transmembrane channel (Song et al. 1996; Valeva et al. 1997). Although no crystal structure is available for the soluble, monomeric form of α-toxin, structural characterization (Meesters et al. 2009) and comparisons with the high-resolution structures of the staphylococcal bi-component leukocidins LukF-PV (Pedelacq et al. 1999) and LukS-PV (Guillet et al. 2004), followed by data based on mutagenesis gave insight into crucial structural elements. In the soluble α-toxin monomer the N-terminal amino latch is folded to the top of the cap domain, and the glycine-rich loop, which would form the stem domain in the transmembrane pore, is stacked against the side of the β-sandwich domain, similar to the amino-terminal latch and stem domains of leukocidins. The α-toxin monomer must go through several conformational changes to form a transmembrane pore. In the initial step of membrane binding both the N- and the C-terminal parts of the toxin seem to be involved in membrane attachment, while the glycine-rich loop turns itself into the middle of the oligomer and becomes excluded from the lipid environment (Olofsson et al. 1988; Panchal and Bayley 1995). In the final step, this central loop extends into a β-hairpin and spans the lipid bilayer. In the insertion process, the N-terminal latch folds down onto the neighboring monomer, clamping the upper crown of the cap domains in the oligomer into a tight and rigid structure (Song et al. 1996). Insertion leads to major conformational changes in all parts of the α-toxin molecule as shown by changes in the cleavage pattern of pronase (Vecsey-Semjen et al. 1997). Conformational changes facilitating membrane binding and insertion might be triggered by acidification of the medium (Forti and Menestrina 1989; Harshman et al. 1989; Vecsey-Semjen et al. 1996). In planar lipid bilayers a lower pH enhanced both channel conductivity and anion selectivity (Krasilnikov and Sabirov 1989). In vivo, pH reduction due to inflammatory processes triggers α-toxin to exert its cytotoxic action intracellularly at far lower concentrations than hitherto assumed. Oligomerization can also occur spontaneously in solution, although with a low efficiency (Ikigai and Nakae 1987; Jayasinghe et al. 2006).

We have shown that naturally occurring α-toxin fragments retain their membrane binding ability and that they intoxicate mouse adrenocortical Y1 cells. All five isolated toxin fragments (Kwak et al. 2010) bound to RRBC membranes and all fragments with intact C terminals formed oligomers, although only the 32-kD fragment, lacking the first 8 aa from its N-terminal latch, was able to irreversibly intoxicate Y1 cells and induce nucleotide release.

Our results are in agreement with previously published data on a comprehensive set of N-terminal truncation mutants (Jayasinghe et al. 2006; Vandana et al. 1997). The authors showed that truncation of the N terminal led to α-toxin species with considerable activity on RRBC and deletion of 11 residues was well tolerated (Jayasinghe et al. 2006). We could not distinguish whether our 31-kD fragment, lacking only 13 aa at the N terminal, was not able to go through the final conformational changes required for channel formation or whether the inner diameters of the transmembrane channels were too small and thereby not permissive for nucleotides. Also, our results on the 26-kD fragment's membrane binding ability were in agreement with previously published data (Walker et al. 1992). In the set of truncation mutants N-terminal deletions did not abolish membrane binding in the monomeric form, and the α-toxin mutants up to 23 aa deletions could still oligomerize on RRBC membranes but did not lyse the cells anymore (Jayasinghe et al. 2006). The isolated 26-kD fragment did form oligomers on RRBC, though. The process of assembly and oligomerization could be a different one, as the 26-kD fragment formed decamers and dodecamers on RRBC membranes (Kwak et al. 2010). It is possible that deletions longer than 23 aa at the N terminal led to inactive species, but activity was regained after further shortages as seen in the case of mutants missing 17–19 aa. While these species were found to be inactive, mutants with longer deletions, missing 20–22 aa from their N terminal, regained activity and were able to lyse RRBC (Jayasinghe et al. 2006).

Our 32.5-kD fragment, lacking five residues from its C terminal, bound to RRBC membranes but failed to form oligomers. Previously C-terminal truncation mutants were reported to bind as monomers on RRBC and undergo a conformational change resulting in occlusion of the protease-sensitive loop, which makes the stem domain (Walker et al. 1992). In the crystal structure of the α-toxin heptamer the carboxyl terminal is on the surface in an

exposed position. Consequently, it is not involved in monomer–monomer interactions and not expected to interfere with the oligomerization process. Further experiments revealed that deletion at the carboxyl terminal leads to a molten-globule-like conformation, loosening up the tertiary structure, and exposure of hydrophobic patches on the monomer's surface (Sangha et al. 1999). This finding explains the membrane attachment of 32.5-kD fragment monomers. The aforementioned studies demonstrate that, in contrast to N-terminal truncations or proteolytic degradations, loss of C-terminal residues might lead to perturbations in the fragment's native folded state. Previously, the existence of nonlytic oligomers was observed both on human granulocyte membranes (Valeva et al. 1997) and on artificial liposome membranes (Vecsey-Semjen et al. 1996). In the latter case, conformational change from the oligomeric to the transmembrane state could be induced by acidification of the medium and/or use of negatively charged phospholipids, where the local pH is expected to be lower than the bulk pH, since the negatively charged head groups give rise to an electrical surface potential that in turn decreases the pH at the membrane surface (Vaz et al. 1978). We applied the latter system to study pore formation of four naturally occurring α-toxin fragments, with special attention to the 26-kD fragment: we induced conformational changes by acidification of the medium and measured the efficiency of pore formation by chloride release from egg-phosphatidyl glycerol (EPG) vesicles. The aim of this was article is to study the relative channel-formation abilities of the spontaneously occurring α-toxin fragments and the relative roles of the N and C terminals.

Materials and Methods

Preparation of Full-Length α-Toxin and Fragments

Staphylococcus aureus strain Wood 46 was cultivated in Brain-Heart Infusion (BHI; GIBCO) medium without the addition of antibiotics in a bench-top fermentor. The α-toxin and fragments were purified from the culture supernatant by cation-exchange chromatography in a sodium acetate buffer (10 mM sodium acetate, pH 5) as previously described (Lind et al. 1987; Kwak et al. 2010), and absorption was measured at 280 nm, based on an optical density of 1.8 for a 1 mg/ml solution of α-toxin and by the Protein Microassay procedure (Bio-Rad).

Preparation of EPG Liposomes

Large unilamellar vesicles were prepared by reverse-phase evaporation as previously described (Gorvel et al. 1991; Szoka and Papahadjopoulos 1978). Liposomes were prepared in buffer of 20 mM HEPES, 100 mM KCl, pH 7.4, with the addition of 1.5 mg/ml 6-methoxy-*N*-(3-sulfopropyl)quinolinium (SPQ). The suspension was extruded first through a 0.4-μm and then through a 0.2-μm polycarbonate filter (Nucleopore) and gel-filtrated on a column (PD 10 column; Pharmacia) equilibrated with the same buffer to remove the extravesicular dye. Maximal release from large unilamellar vesicles was induced by Triton X-100 and used as 100% release in the experiments.

Measurements of Chloride Efflux

Experiments were carried out on a Perkin-Elmer LS 5B spectrometer with a spectral bandwidth of 5 nm for both excitation and emission. The dye was excited at 350 nm and emission was recorded at 422 nm as previously described (Vecsey-Semjen et al. 1996). Experiments were performed at 25°C under continuous stirring. Liposomes were diluted to a final concentration of 60 μM (alt: 50 μg/ml) in buffers containing 100 mM KNO_3:20 mM HEPES at pH 7.0, 20 mM MES at pH levels 4.0–6.0, or 20 mM citric acid-*di*-sodium hydrogen phosphate at pH 3.5. The α-toxin and 32.5-, 32-, 31-, and 26-kD fragments were added to the reaction mixture to a final concentration of 200 ng/ml. Opening of effective channels was inhibited by 1 or 4 mM zinc sulfate ($ZnSO_4$) in the medium. Preopened channels were closed by addition of 1 mM $ZnSO_4$ and reopened by the addition of 2 mM EDTA.

Estimation of Membrane Inserted Oligomers Bound to EPG Vesicles

After chloride efflux measurements at pH 4.5, vesicles were sedimented by ultracentrifugation at 4°C for 60 min at 80,000 rpm (Beckman benchtop 64R), solubilized in sample buffer, and run on an 8% SDS-polyacrylamide gel. To prevent disruption of the oligomer, samples were kept on ice. For estimation of oligomers formed at the different pH values, at the end of each chloride efflux measurement the vesicles were recovered by discontinuous sucrose gradient ultracentrifugation. Briefly, for high-density sucrose 260-μl samples were mixed with 540 μl of 61% sucrose and transferred to the bottom of 3-ml centrifuge tubes. Carefully 1700 μl of 35% sucrose was layered on top, followed by 900 μl of 17.5% and 600 μl of 10% sucrose. The tubes were finally filled up with 400 μl buffer and EPG vesicles separated from unbound toxin fragments by ultracentrifugation at 4°C for 60 min at 35,000 rpm (Beckman, benchtop 64R) as previously described by Gorvel et al. (1991). Vesicles were recovered from the top of the 35% sucrose layer as a white fluffy band and analyzed by SDS-polyacrylamide gel electrophoresis under nonboiling conditions.

Hemolytic Assay

For the determination of hemolytic activity RRBC were washed 3 times with PBS and sedimented by gentle centrifugation. For determination of 100% hemolysis, a 100 µl RRBC suspension was centrifuged, the supernatant removed, and the erythrocytes lysed in 200 µl distilled water. A standard curve was created by serial dilution of the standardized RRBC suspension from 0.1% to 1% at 0.1% intervals in TBS as previously described (Kanclerski and Mollby 1987). For determination of hemolytic activity, 10 µl of 1 µg/ml intact α-toxin or fragments was diluted with 90 µl TBS, pH 7.4, containing 1% bovine serum albumin (BSA) buffer in the first well of each row of a 96-well microtiter plate (Greiner Bio-One). A protein concentration gradient was created by serial twofold dilutions in the same buffer across each row. To each 100 µl toxin-containing well, 100 µl of washed rabbit or human erythrocyte in 1% suspension was added and the plates were incubated for 30 min at 37°C. After cooling, the settled erythrocytes were carefully resuspended by pipetting and the density of the remaining cells was measured as the decrease in light scattering at 620 nm in a microplate reader (Labsystems Integrated EIA Management System). For determination of the pH dependence of the hemolytic activity, erythrocytes were resuspended in 145 mM NaCl buffered with 50 mM citric acid-*di*-sodium hydrogen phosphate in the pH range 4.5–7.5 in steps of 0.5 pH unit. The same buffers were used for serial dilutions of protein samples. The hemolytic titer (HU) was defined as the amount of active hemolysin present in the dilution and was interpolated as the inverted value of a fictive dilution corresponding to exactly 50% hemolysis.

Spontaneous Oligomerization in Aqueous Solution

Samples of α-toxin and fragments were diluted in TBS, pH 7.4, to concentrations of 0.5 mg/ml (32.5- and 32-kD fragments) and 1 mg/ml (intact α-toxin and 26-kD fragment) and kept at 37°C for 4 h, during which time they were repeatedly mildly vortexed (Ikigai and Nakae 1987). Aliquots of 5 and 10 µl were mixed with 4 × SDS-sample buffer. The 5-µl samples were heated to 80°C for 5 min and the heated and unheated samples were analyzed in parallel by SDS-PAGE.

Results

Purification of α-Toxin and Fragments

The intact toxin and four α-toxin fragments have been purified from the late *lag* phase of *Staphylococcus aureus* Wood 46 culture supernatant and identified by N-terminal sequencing (Kwak et al. 2010). The largest 32.5-kD fragment has an intact N terminal but lost 5 aa from its C terminal, as a result of proteolytic degradation by staphylococcal V8 enzyme. Two fragments, of sizes 32 and 31 kD, lost 8 and 12 aa, respectively, of their N-terminal ends. The 26-kD fragment (aa 72–293), the result of cleavage with V8 enzyme and/or aureolysin and further degradation of the N-terminal part of the intact α-toxin, could be recovered in high amounts. The isolated fragments bind specific antibodies and bind to RRBC membranes (Kwak et al. 2010).

Chloride Release from SPQ-Filled EPG Vesicles

We have previously shown that α-toxin has to go through partial unfolding for membrane binding and channel formation to occur and this partial unfolding could be triggered by acidification of the medium (Vecsey-Semjen et al. 1996). To study channel formation by α-toxin fragments, we employed similar conditions that were optimal for channel formation by α-toxin, such as EPG large unilamellar vesicles, with the combined advantage of having a mixture of saturated and unsaturated lipids with negatively charged head groups, which gave rise to an electrical surface potential that decreased the pH at the membrane surface (Vaz et al. 1978; Vecsey-Semjen et al. 1996; Winiski et al. 1988). We studied channel formation by monitoring chloride release from vesicles containing the chloride-sensitive dye SPQ. We have previously shown that the chloride efflux observed was not the result of membrane fusion induced either by α-toxin or by low pH (Vecsey-Semjen et al. 1996). In the present study we presumed that none of the isolated fragments induced membrane fusion either. Also, we ensured that in our experimental setting the chloride efflux induced by the fragments was dose dependent. All isolated α-toxin fragments induced chloride release in a pH-dependent manner from EPG vesicles with kinetics similar to that of the intact α-toxin. However, the efficiency of channel formation varied greatly. α-Toxin induced maximal chloride release (91%) at pH 4.5 (Vecsey-Semjen et al. 1996) (Fig. 1a); this maximum shifted to pH 4.0 for the 32.5-kD fragment and the efficiency of channel formation dropped to 38% (Fig. 1a). Surprisingly, the 32-kD fragment, lacking only 8 aa from its N terminus, was only slightly more active, as we observed maximal release at pH 4.5 with an efficiency of 46% (Fig. 1b). Channel formation by the 31-kD fragment was most effective at pH 4.75 and induced as much as 53% release (Fig. 1c). The 26-kD fragment behaved much as the intact α-toxin, as it induced 82% chloride release at pH 4.5 (Fig. 1d). We compared the channel-forming efficiency of the four different toxin fragments in our study by

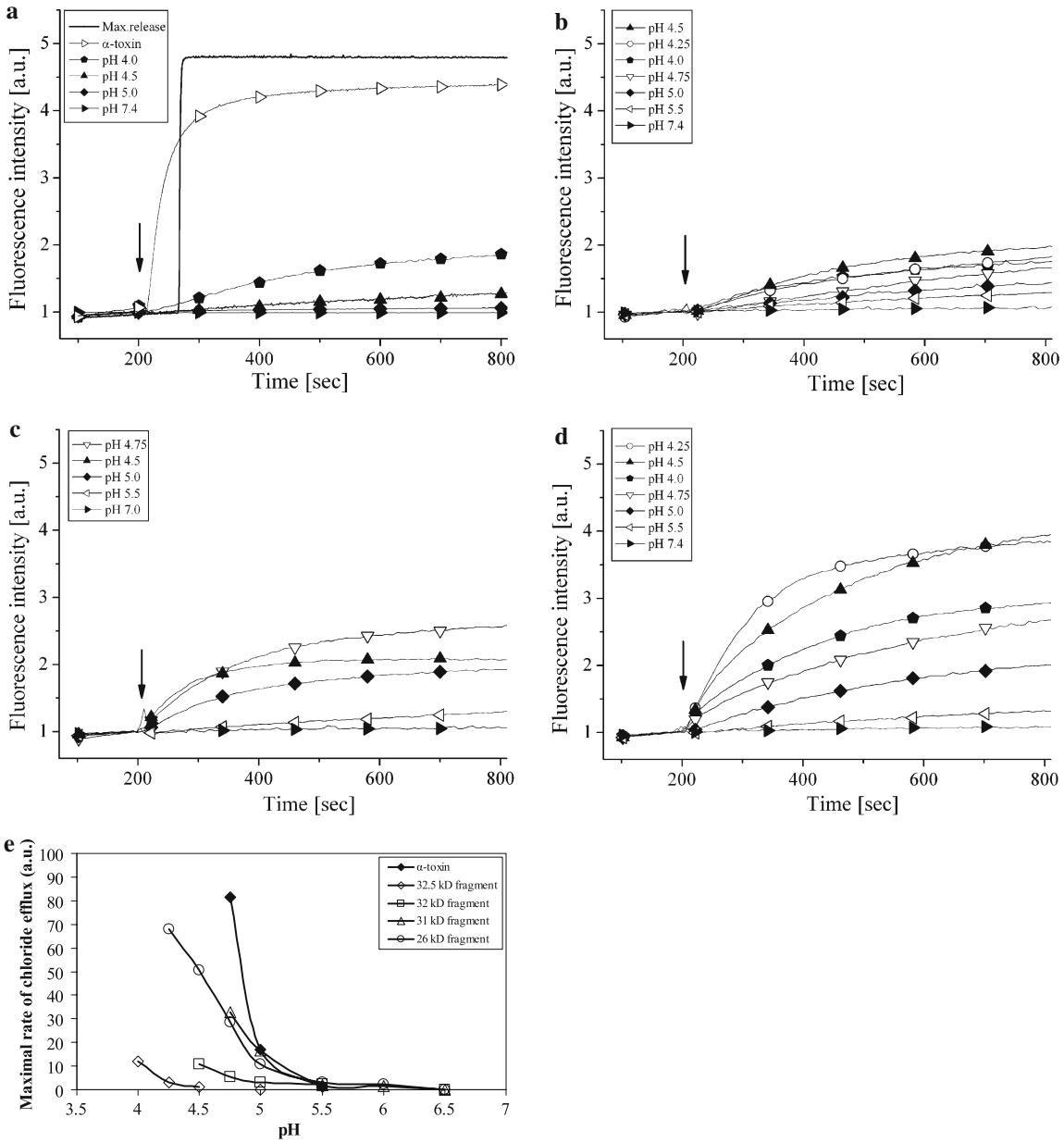

Fig. 1 Effect of pH on α-toxin and α-toxin fragment-induced chloride efflux from SPQ-filled EPG liposomes. Channel formation was measured as the change in fluorescence intensity of the chloride-sensitive dye SPQ upon channel formation. Chloride efflux from liposomes was measured at various pH values (25°C) in 100 mM KNO_3 buffered with 20 mM MES. The time point at which α-toxin or toxin fragment was added is indicated by an *arrow*. Maximal release after the addition of Triton X-100 and release after the addition of full-length α-toxin are shown for comparison. Channel formation by a 32.5-kD α-toxin fragment (**a**), by a 32-kD fragment (**b**), by a 31-kD fragment (**c**), and by a 26-kD fragment (**d**). The maximal rate of α-toxin fragment-induced chloride efflux from EPG vesicles was plotted as a function of buffer pH. α-Toxin-induced efflux is shown for comparison (**e**)

plotting the maximal rate of chloride efflux as a function of pH. It clearly appears that intact α-toxin was most sensitive to the bulk pH followed by the 26-kD fragment (Fig. 1e). Generally, all fragments were more protonation dependent for channel formation and chloride efflux occurred at lower pH values than for the intact toxin. To exclude the possibility that chloride efflux was a result of nonspecific membrane damage, caused by protein binding, we investigated if the release could be inhibited by zinc, which has been shown to block the α-toxin channel (Menestrina 1986). Opening of channels could be inhibited by 1 mM zinc in the medium (data not shown). Also, preopened channels could be closed by addition of zinc in the medium and the effect could be reversed by addition of the chelating agent EDTA (2 mM). The closure of the preformed channels could be the result of steric hindrance caused by

the metal ions bound to the entrance of the channel or a minor conformational change induced.

Oligomerization on EPG Membranes

Correct oligomerization is a prerequisite for channel formation (Valeva et al. 1995). To see if there was a correlation between oligomer formation on EPG membranes and chloride release, we determined the amount of oligomers formed by the various fragments on the liposome membranes. Therefore, at the end of each chloride efflux measurement, vesicles were sedimented by ultracentrifugation and analyzed by SDS-PAGE without heating the samples. Previously we have shown that the amounts of α-toxin oligomers formed were very similar at all pH values studied (Vecsey-Semjen et al. 1996). Similarly, the 32- and 31-kD fragments, missing 8 and 12 aa, respectively, from N-terminal amino latches formed oligomers at all pH values, but with a much lower efficiency (data not shown). The 26-kD fragment formed oligomers of at least three different sizes, probably as the result of oligomers formed by various numbers of protomers. Furthermore, the efficiency of oligomer formation at pH 4.5 was even more effective than that of intact α-toxin (Fig. 2a). Surprisingly, we were not able to detect any oligomers formed by the 32.5-kD fragment under neutral conditions. Despite the fact that we found only monomers sedimented with the vesicles, the fragment induced considerable chloride efflux at pH 4.0. Next we investigated whether oligomer formation was strongly pH dependent or whether release from vesicles could be the consequence of membrane perturbation caused by the 32.5-kD monomers. After chloride efflux measurement at each pH, vesicles were floated up on a discontinuous sucrose gradient and the fluffy lipid layer analyzed on an SDS gel (Fig. 2b). In contrast to intact α-toxin and the 32- and 31-kD fragments, there seemed to be a a strong correlation between oligomer formation and chloride efflux for the 32.5-kD monomers. Two high molecular weight bands, representing oligomers, could be seen at pH 4.0, the same pH value at which chloride efflux could be measured. In the case of the 32.5-kD fragment, pH seems to have a significant effect on the oligomerization process, possibly by inducing further conformational changes in the monomer that trigger oligomerization.

Hemolytic Activity

Previous experiments on EPG liposomes showed that channel formation of the isolated α-toxin fragments was highly pH dependent. In the next step we investigated whether hemolysis could also be triggered by lowering of the pH and tested the hemolytic activity of the fragments in the pH range 4.5–7.5 on RRBC. Intact α-toxin optimally lysed RRBC under neutral physiological conditions, pH 7.0. With

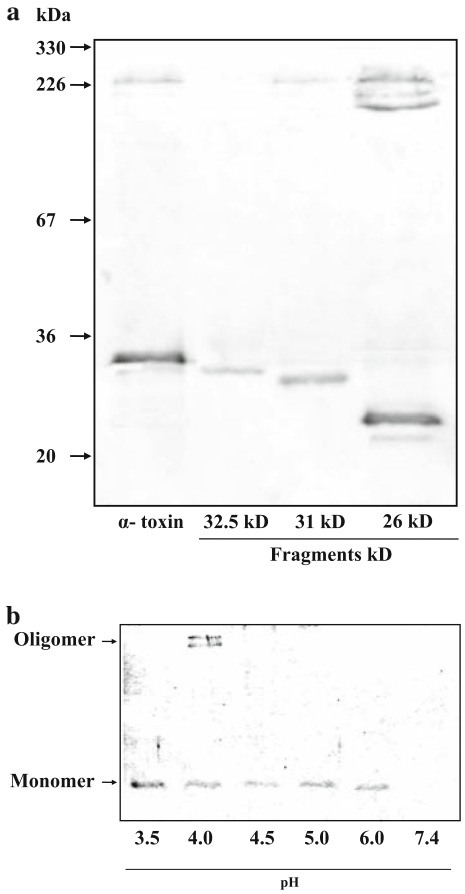

Fig. 2 Oligomers formed by α-toxin and α-toxin fragments detected on EPG vesicle membranes. After chloride efflux measurements at pH 4.5, vesicles were sedimented by ultracentrifugation, solubilized in sample buffer, and run on an 8% SDS-polyacrylamide gel. To prevent disruption of the oligomers, samples were not boiled. *Arrows* show the position of oligomeric and monomeric α-toxin (**a**). Oligomerization and channel formation by the 32.5-kD fragment: after each chloride efflux measurement, the vesicles were recovered by discontinuous sucrose gradient ultracentrifugation and analyzed by SDS-PAGE under nonboiling conditions (**b**)

a decrease in pH, the toxin's hemolytic activity decreased, leveling out at pH 6.0 into a second, minor peak at pH 5.5. Consistent with this result, the dual mechanism of α-toxin binding to RRBC membranes was previously described (Hildebrand et al. 1991). At pH 7.0, α-toxin binds to specific binding sites at low concentrations, forms transmembrane channels, and lyses RRBC with a high efficiency. Acidification of the medium led to a loss of binding specificity. The second hemolytic peak, at pH 5.5, reflects nonspecific binding to lipid moieties and lysis (Fig. 3a). Fragments with an intact C terminal (32, 31, and 26 kD) showed a single hemolytic peak at pH 5.5, which coincided with the minor peak of the intact toxin (Fig. 3a). In contrast to previous observations, where α-toxin deletion mutants of up to 12 aa had considerable hemolytic activity (Jayasinghe et al. 2006), the loss of only 8 aa from the N terminal resulted in an

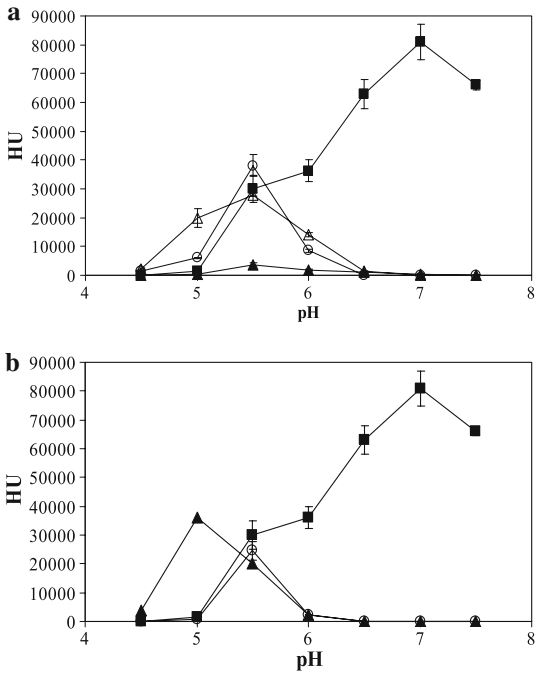

Fig. 3 Effect of pH on the hemolytic activity of α-toxin and α-toxin fragments. **a** Washed rabbit erythrocytes (RRBC) were resuspended in 150 mM NaCl buffered with 50 mM citric acid-*di*-sodium hydrogen phosphate of various pH values. The hemolytic activity of the serially diluted samples was read after 30 min of incubation (37°C) in a vertical spectrophotometer at 620 nm. The reference value for 50% lysis was obtained by mixing 50 µl of RRBC suspension with 150 µl of diluting buffer. Hemolysis of α-toxin (*filled square*), the 32-kD fragment (*open circle*), the 31-kD fragment (*open triangle*), and the 26-kD fragment (*filled triangle*) at different pH values. **b** pH dependence of α-toxin (*open circle*) and the 32-kD fragment (*filled triangle*) on human erythrocytes (HRBC). For comparison, α-toxin hemolysis on RRBC (*filled square*) is also shown

inactive fragment at pH 7.0 in our assay. The explanation for this discrepancy might be the short assay time, as an increase in the initial lag time was previously observed (Jayasinghe et al. 2006; Vandana et al. 1997). We evaluated hemolysis after only 30 min, while the truncated mutants were observed for over 2 h. According to our results, with the loss of the N terminal, the 32- and 31-kD fragments' ability to lyse RRBC at neutral pH practically ceased and the 26-kD fragment's hemolytic activity dropped to 0.6% of that of the intact α-toxin at pH 7.0. In contrast, at pH 5.5, the 32-kD fragment lysed RRBC more efficiently than intact α-toxin (127%) (Fig. 3a). The largest isolated 32.5-kD fragment, lacking only five residues from the C terminus, had no hemolytic activity and could not be activated by changes in the buffer pH (Data not shown). Previous reports described the C-terminal deletion mutants as nonhemolytic, despite the fact that they readily formed multimers (Sangha et al. 1999; Walker et al. 1992). Binding of α-toxin to RRBC initially involves specific binding sites. In contrast, toxin binding to HRBC is nonspecific. To clarify whether the fragments' diminished hemolytic activity and the shift in maximum to lower pH could be the result of their inability, or loss of ability, to bind to specific receptors on the RRBC, we determined the α-toxin fragments' hemolytic activity on HRBC. Only the 32-kD fragment could lyse HRBC at pH 5.5 with an efficiency (86%) similar to that of α-toxin. Also, maximal hemolysis was measured after further acidification at pH 5.0 (Fig. 3b). None of the other isolated α-toxin fragments were hemolytic on HRBC, at any pH. Our results show that, although the N terminal of α-toxin is not required for pore formation on lipid membranes, proteolytic degradation demolished specific binding to RRBC and reduced activity. By acidification of the medium we could restore the fragments' hemolytic activity, though only partially.

Oligomerization in Solution

We then investigated whether the diminished channel-forming abilities of the fragments was a consequence of premature oligomerization, since both the amino latch and the C terminus shield hydrophobic patches. In fact, the

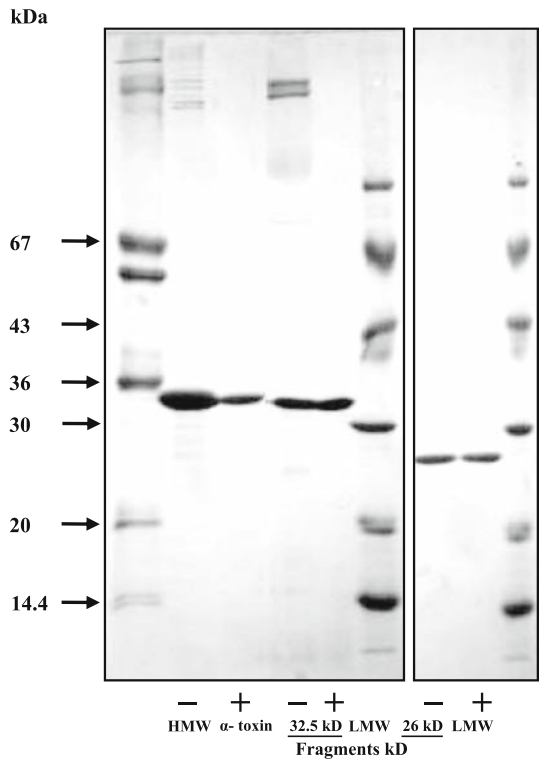

Fig. 4 Spontaneous oligomerization in solution. Samples (1 mg/ml) of α-toxin and the 32.5-kD toxin fragment were incubated in TBS, pH 7.4, at room temperature (24°C) for 6 h. During incubation the samples were mildly repeatedly vortexed. To prevent disruption of the oligomers, two-thirds of the final sample (70 µl) was applied without heating (−), while the other one-third (35 µl) was heated to 80°C for 5 min (+) before electrophoresis. HMW, high molecular weight standards (200,000, 116,250, 97,400, 66,200, 45,000); LMW, low molecular weight standards (97,400, 66,200, 45,000, 31,000)

32.5-kD fragment formed oligomers readily in solution much more efficiently than the intact toxin (Fig. 4). Also, some of our original samples employed in previous experiments had contaminations of preformed oligomers, although the samples were always kept on ice during the experiments and repeated thawings were avoided (data not shown). After extended incubation at 37°C and repeated vortexing, a double band of oligomers, slightly smaller than the oligomeric bands of the intact toxin, could be seen (data not shown). The 32- and 31-kD fragments formed oligomers of uniform sizes but with a very low efficiency. The 26-kD fragment did not form any oligomers in solution, even when incubated for longer periods such as overnight (Fig. 4).

Discussion

Understanding of the membrane-binding and channel-forming mechanisms of staphylococcal α-toxin greatly enhanced our possibilities to construct useful tools for biotechnological applications (Bayley and Cremer 2001). Therefore it is important to clarify the assembly mechanism and channel function of α-toxin. Also, α-toxin plays a major role in *Staphylococcus aureus* infections as a bacterial determinant, associated with changes in virulence (Kahl et al. 1996). In both aspects, knowledge about α-toxin fragments, occurring after cleavage with co-expressed proteases, may contribute to the production of membrane channels with new properties and/or the construction of new antibacterial treatments.

Here we have presented four spontaneously occurring α-toxin fragments that retain their oligomerizing and channel-forming ability. Fragments with an intact C terminal, but missing more than 8 aa from their N-terminal part, required acidification of the medium to insert and form channels in EPG vesicles. In a model system it was previously shown that channel formation, but not oligomerization, on the liposome membranes was protonation dependent (Vecsey-Semjen et al. 1996).

A model for membrane insertion and pore formation is generally accepted: the membrane insertion of the central loop, encompassing about 15 residues (Song et al. 1996; Valeva et al. 1996), underlies pore formation. Part of the energy of oligomerization is probably coupled to the process in which the central loop is driven into the lipid bilayer. Low pH and protonation drive the necessary conformational changes that result in pore formation and, consequently, release of chloride from EPG vesicles.

Induction of chloride release from EPG vesicles by the 26-kD α-toxin fragment indicates the formation of effective transmembrane pores. These pores were built by a varying number of protomers (Fig. 2a), resulting in large multimers of different sizes. The inner diameter of the transmembrane channels is likely to be smaller than the α-toxin channels because previously we found that they are not permeable to nucleotides (Kwak et al. 2010). While intact α-toxin forms heptamers in lipid bilayers, the 26-kD fragment oligomerized into decamers and dodecamers on RRBC membranes and octamers, nonamers, and decamers on EPG membranes, more similar to leukocidins (Menestrina et al. 2003; Miles et al. 2006). It seems that not only does the oligomerization process of the 26-kD fragment lead to multimers of varying numbers of subunits, but also the process is membrane and lipid composition dependent. Thus, the first 71 aa of α-toxin are not essential for membrane binding and pore formation to occur but are needed for the formation of uniform oligomers. It is of considerable importance to analyze the 26-kD fragment's properties, as it seems to be the smallest channel-forming entity of α-toxin described so far. Truncation of residues 1–71 removes a large part of the native protomer-protomer interface of the full-length heptamer (Fig. 5). This suggests

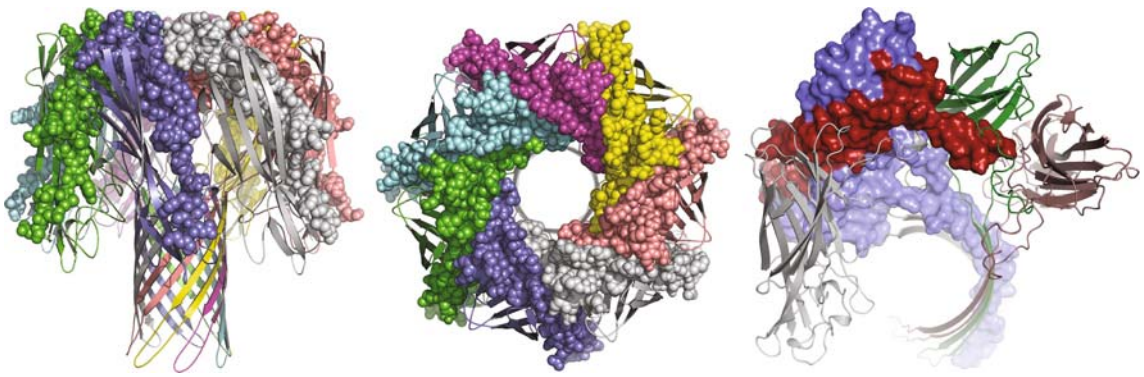

Fig. 5 Structural features of the heptameric pore and the N-terminal segment. *Left*, *middle* structure of the intact α-toxin heptamer (Song et al. 1996). Each subunit is shown in a *different color*. Amino acids 1–71, absent in the 26-kD fragment, are shown as *spheres*. *Right* Molecular surface of one protein monomer; the surface contributed by amino acids 1–71 is shown in *red*, and three interacting monomers in the heptameric pore are also shown. The figure shows the major role that the N-terminal segment plays in protomer interaction in the heptameric pore and the drastic differences that must occur in the 26-kD fragment when residues 1–71 are absent

that the protomer interactions in the cap domain of the 26-kD fragment oligomers must be fundamentally different from those in the heptamers of the full-length protein. Moreover, while the full-length protein forms heptamers, the 26-kD fragment forms multimers of different sizes, indicating that the truncation affects both the mechanism of oligomer formation and preference for various multimeric states. Even though higher multimers could be expected to form larger pores, one must also take other structural features into account. First, the truncated cap domain is significantly smaller than that of the full-length protein. Second, the different interactions between the protomers in the 26-kD fragment multimer compared to the full-length heptamer will influence the geometry of the cap domain multimer and are likely to influence the permeability properties. In the full-length heptameric structure the narrowest part is in the interface region between the stem and the cap domains; structural changes in this area are thus likely to affect permeability of the membrane channel. The triangle region, connecting the solvent-exposed β-sandwich structure with the membrane inserted stem domain (Meesters et al. 2009; Song et al. 1996), was shown to play a crucial role in protomer–protomer interactions between intact α-toxin monomers and was suggested to play a role in the conformational changes leading to an open channel. The fact that the oligomers formed by the 26-kD fragment induce chloride release but very little nucleotide release (Kwak et al. 2010) suggests that these possess a more narrow channel than the full-length protein. The smaller size of the pore is most likely caused by the now much smaller cap domain packing to form a smaller central pore. This will also influence the relative orientation of the cap domain to the stem domain, which may induce additional structural changes throughout the channel.

Similarly to the 26-kD fragment, the 31-kD fragment formed ion-transmissible channels in EPG vesicle membranes. Though we could see only one single band in Coomassie-stained SDS-gel corresponding to heptamers, we cannot exclude the formation of hexamers and octamers in much lesser amounts. On RRBC membranes, all three oligomeric species were formed (Kwak et al. 2010). The maximal release from EPG vesicles induced by the 31-kD fragment was only 53%, which corresponds well to previous results measured on planar lipid bilayers. Surprisingly, the 32-kD fragment induced only 46% maximal release, despite the fact that this fragment alone could cause irreversible intoxication and nucleotide release from Y1 cells (Kwak et al. 2010). The effectivity of channel formation was comparable (43.6 and 46%, respectively). In the Luk pore, F and S subunits are arranged in an alternating fashion to form an octamer (Miles et al. 2002). Although the F and S proteins share approximately 27% identity with each other and no more than 30% identity with α-toxin, the similar structural features of these proteins make the set of Luk monomers and the α-toxin oligomer a powerful kit for studies of pore formation. In contrast to the X-ray studies showing a strictly heptameric stoichiometry for oligomers formed in deoxycholate micelles (Song et al. 1996), hexamers were found in phospholipids bilayers by atomic force microscopy studies (Czajkowsky et al. 1998). Furthermore, an alternative oligomeric arrangement, based on observation of structures of different sizes in EM studies, was suggested, which may be of relevance to the mechanisms by which α-toxin damages eukaryote cells (Ellis et al. 1997; Hebert et al. 1992).

All three isolated fragments with an intact C terminal had considerable hemolytic activity on RRBC and some on HRBC under acidic conditions. The fact, that the loss of eight N-terminal amino acids led to strongly diminished haemolytic activity on RRBC at neutral pH, is surprising. Our results also reveal one more fact of the nature of the elusive binding sites on RRBC membranes: it seems to require a discontinuous epitope on the surface of intact α-toxin which is sensitive to minor deletions and conformational changes. In the light of our results, reduced hemolytic activity of the fragments can only be explained by loss of the ability to bind specifically to clustered phosphocholine head groups on the RRBC surface (Valeva et al. 2006). Our present results support the dual mechanism of α-toxin RRBC hemolysis as it has been previously described (Hildebrand et al. 1991). α-Toxin reached its maximal hemolytic activity on RRBC at pH 7.4, compared to pH 5.5 on HRBC, i.e., at the same pH value at which we observed a minor peak. Also, we measured maximal hemolytic activity for the fragments at the same pH. The second, common peak mirrors nonspecific binding to clustered phospholipid head groups and disruption of the RRBC membrane for α-toxin and fragments. The phenomenon might be a consequence of α-toxin going through minor conformational changes at acidic pH, thereby losing essential epitopes for receptor binding. Similarly, the fragments' inability to attach to specific binding sites on RRBC might be explained by minor conformational changes due to loss of the N-terminal end and, consequently, loss of specificity as human erythrocytes lack surface receptors (Hildebrand et al. 1991). Alternatively, the specific receptors at the RRBC surface are sensitive to acidification of the medium.

Proteolytic degradation in the amino latch had little influence on the 32-kD fragment's capacity to irreversibly intoxicate Y1 cells and induce nucleotide release. In contrast, the fragment's ability to lyse RRBC was drastically diminished. This result was both unexpected and intriguing. The N-terminal latch of α-toxin had never been supposed to be the binding site either to RRBC or lipid membranes. Also, the 32.5-kD fragment, with an intact N terminal, failed to bind and lyse RRBC. Thus, proteolytic cleavage at the N-terminal of intact α-toxin results in fragments that are not biologically inactive, but highly

dependent on protonation for their action. The fact that the fragments' channel-forming ability was improved by a slightly acidic pH in experiments with erythrocytes, while the same changes in buffer pH had no effect on nucleotide release from Y1 cells, can be explained by differences between the erythrocyte and the nucleated cell membranes.

The isolated 32.5-kD fragment (1–288 aa), lacking the C terminal, has a tendency to aggregate in the absence of membranes (Fig. 4). Under acidic conditions, the fragment binds to membranes but forms detectable oligomers on EPG membranes only at pH 4.0, i.e., at the same pH at which chloride release could be measured. Because no traces of oligomers were obtained with the 32.5-kD fragment either on RRBC membranes (Kwak et al. 2010) or on EM images (data not shown) under neutral conditions, we can only conclude that the fragment adapts a partially unfolded structure as the near UV-CD spectrum previously indicated (Sangha et al. 1999). Protonation due to acidification of the medium and negatively charged phospholipid head groups, such as PG, seems to lead to further unfolding into a membrane-insertion-competent molten globule state and so enable it to form transmembrane channels (van der Goot et al. 1991). The channel-forming process was protonation dependent for all isolated fragments, in agreement with previous results with intact α-toxin (Forti and Menestrina 1989; Harshman et al. 1989; Vecsey-Semjen et al. 1996, 1997).

We have shown that native α-toxin goes through proteolysis by simultaneously expressed staphylococcal exoproteases (Kwak et al. 2010). The obtained fragments, cleaved at the N-terminal end, are able to go through oligomerization and after conformational changes, triggered by protonation, can form transmembrane pores. The process may have implications in the pathophysiological role of α-toxin in staphylococcal infections. *Staphylococcus aureus* can invade, survive, and replicate in many different cell types (Jarry et al. 2008; Menzies and Kourteva 1998). Phagocytosed bacteria are usually eliminated in the lysosome by hydrolytic enzymes. In contrast, *S. aureus* escapes from the phagolysosome by activating RNA III transcription and exotoxin expression (Novick 2003). Thus, not only α-toxin expression but also toxin insertion into the endosome membrane is triggered by low pH (Jarry et al. 2008). In this process naturally occurring fragments may play a role, as they are biologically active and may enhance the tissue damage caused by the bacteria.

Acknowledgment We express our gratitude to Patricia Colque-Navarro for her guidance and patience with us in endless discussions on *Staphylococcus aureus*.

Appendix

See Fig. 6.

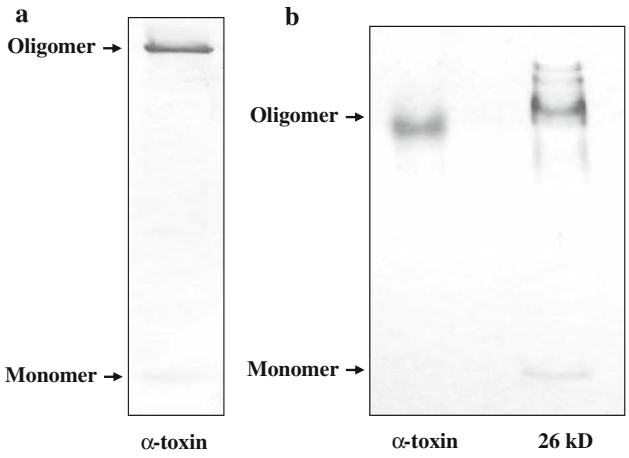

Fig. 6 Comparison of SDS-PAGE (**a**) with BN-PAGE (**b**) for the analysis of α-toxin and 26-kD fragment

References

Bayley H, Cremer PS (2001) Stochastic sensors inspired by biology. Nature 413:226–230

Czajkowsky DM, Sheng ST, Shao ZF (1998) Staphylococcal alpha-hemolysin can form hexamers in phospholipid bilayers. J Mol Biol 276:325–330

Ellis MJ, Hebert H, Thelestam M (1997) *Staphylococcus aureus* alpha-toxin: characterization of protein/lipid interactions, 2D crystallization on lipid monolayers, and 3D structure. J Struct Biol 118:178–188

Forti S, Menestrina G (1989) Staphylococcal alpha-toxin increases the permeability of lipid vesicles by cholesterol-dependent and pH-dependent assembly of oligomeric channels. Eur J Biochem 181:767–773

Gorvel JP, Chavrier P, Zerial M, Gruenberg J (1991) rab5 controls early endosome fusion in vitro. Cell 64:915–925

Guillet V, Roblin P, Werner S, Coraiola M, Menestrina G, Monteil H, Prevost G, Mourey L (2004) Crystal structure of leucotoxin S component—new insight into the staphylococcal beta-barrel pore-forming toxins. J Biol Chem 279:41028–41037

Harshman S, Boquet P, Duflot E, Alouf JE, Montecucco C, Papini E (1989) Staphylococcal alpha-toxin—a study of membrane penetration and pore formation. J Biol Chem 264:14978–14984

Hebert H, Olofsson A, Thelestam M, Skriver E (1992) Oligomer formation of staphylococcal alpha-toxin analyzed by electron-microscopy and image-processing. FEMS Microbiol Immunol 105:5–12

Hildebrand A, Pohl M, Bhakdi S (1991) *Staphylococcus aureus* alpha-toxin—dual mechanism of binding to target cells. J Biol Chem 266:17195–17200

Ikigai H, Nakae T (1987) Interaction of the alpha-toxin of *Staphylococcus aureus* with the liposome membrane. J Biol Chem 262:2150–2155

Jarry TM, Memmi G, Cheung AL (2008) The expression of alpha-haemolysin is required for *Staphylococcus aureus* phagosomal escape after internalization in CFT-1 cells. Cellular Microbiology 10:1801–1814

Jayasinghe L, Miles G, Bayley H (2006) Role of the amino latch of staphylococcal alpha-hemolysin in pore formation—a co-operative interaction between the N terminus and position 217. Journal of Biological Chemistry 281:2195–2204

Kahl B, Herrmann M, Everding AS, Koch HG, Becker K, Harms E, Proctor RA, Peters G (1996) Persistent infection with small colony variant strains of *Staphylococcus aureus* in patients with cystic fibrosis. In: 36th Interscience conference on antimicrobial agents and chemotherapy. University of Chicago Press, New Orleans, Louisiana, pp 1023–1029

Kanclerski K, Mollby R (1987) A simple and exact 2-point interpolation method for determination of hemolytic-activity in microtiter plates. Acta Pathol Microbiol Immunol Scand Sect B 95:175–179

Krasilnikov OV, Sabirov RZ (1989) Ion transport through channels formed in lipid bilayers by *Staphylococcus aureus* alpha-toxin. Gen Physiol Biophys 8:213–222

Kwak Y-K, Högbom M, Colque-Navarro P, Möllby R, Vecsey-Semjen B (2010) Biological relevance of natural α-toxin fragments from *Staphylococcus aureus*. J Membr Biol 233:93–103

Lind I, Ahnerthilger G, Fuchs G, Gratzl M (1987) Purification of alpha-toxin from *Staphylococcus aureus* and application to cell permeabilization. Anal Biochem 164:84–89

Meesters C, Brack A, Hellmann N, Decker H (2009) Structural characterization of the alpha-hemolysin monomer from *Staphylococcus aureus*. Proteins 75:118–126

Menestrina G (1986) Ionic channels formed by *Staphylococcus aureus* alpha-toxin—voltage-dependent inhibition by divalent and trivalent cations. J Membr Biol 90:177–190

Menestrina G, Serra MD, Comai M, Coraiola M, Viero G, Werner S, Colin DA, Monteil H, Prévost G (2003) Ion channels and bacterial infection: the case of beta-barrel pore-forming protein toxins of *Staphylococcus aureus*. FEBS Lett 552:54–60

Menzies BE, Kourteva I (1998) Internalization of *Staphylococcus aureus* by endothelial cells induces apoptosis. Infect Immun 66:5994–5998

Miles G, Movileanu L, Bayley H (2002) Subunit composition of a bicomponent toxin: staphylococcal leukocidin forms an octameric transmembrane pore. Protein Sci 11:894–902

Miles G, Jayasinghe L, Bayley H (2006) Assembly of the bicomponent leukocidin pore examined by truncation mutagenesis. J Biol Chem 281:2205–2214

Novick RP (2003) Mobile genetic elements and bacterial toxinoses: the superantigen-encoding pathogenicity islands of *Staphylococcus aureus*. Plasmid 49:93–105

Olofsson A, Kaveus U, Thelestam M, Hebert H (1988) The projection structure of alpha-toxin from *Staphylococcus aureus* in human-platelet membranes as analyzed by electron-microscopy and image-processing. J Ultrastruct Mol Struct Res 100:194–200

Panchal RG, Bayley H (1995) Interactions between residues in staphylococcal alpha-hemolysin revealed by reversion mutagenesis. J Biol Chem 270:23072–23076

Pedelacq JD, Maveyraud L, Prevost G, Baba-Moussa L, Gonzalez A, Courcelle E, Shepard W, Monteil H, Samama JP, Mourey L (1999) The structure of a Staphylococcus aureus leucocidin component (LukF-PV) reveals the fold of the water-soluble species of a family of transmembrane pore-forming toxins. Structure 7:277–287

Sangha N, Kaur S, Sharma V, Krishnasastry MV (1999) Importance of the carboxyl terminus in the folding and function of alpha-hemolysin of *Staphylococcus aureus*. J Biol Chem 274:9193–9199

Song LZ, Hobaugh MR, Shustak C, Cheley S, Bayley H, Gouaux JE (1996) Structure of staphylococcal alpha-hemolysin, a heptameric transmembrane pore. Science 274:1859–1866

Szoka F, Papahadjopoulos D (1978) Procedure for preparation of liposomes with large internal aqueous space and high capture by reverse-phase evaporation. Proc Natl Acad Sci USA 75:4194–4198

Valeva A, Palmer M, Hilgert K, Kehoe M, Bhakdi S (1995) Correct oligomerization is a prerequisite for insertion of the central molecular domain of staphylococcal alpha-toxin into the lipid bilayer. Biochim Biophys Acta 1236:213–218

Valeva A, Weisser A, Walker B, Kehoe M, Bayley H, Bhakdi S, Palmer M (1996) Molecular architecture of a toxin pore: a 15-residue sequence lines the transmembrane channel of staphylococcal alpha-toxin. EMBO J 15:1857–1864

Valeva A, Walev I, Pinkernell M, Walker B, Bayley H, Palmer M, Bhakdi S (1997) Transmembrane beta-barrel of staphylococcal alpha-toxin forms in sensitive but not in resistant cells. Proc Natl Acad Sci USA 94:11607–11611

Valeva A, Hellmann N, Walev I, Strand D, Plate M, Boukhallouk F, Brack A, Hanada K, Decker H, Bhakdi S (2006) Evidence that clustered phosphocholine head groups serve as sites for binding and assembly of an oligomeric protein pore. J Biol Chem 281:26014–26021

van der Goot FG, Gonzalez-Manas JM, Lakey JH, Pattus F (1991) A 'molten-globule' membrane-insertion intermediate of the pore-forming domain of colicin A. Nature 354:408–410

Vandana S, Raje M, Krishnasastry MV (1997) The role of the amino terminus in the kinetics and assembly of alpha-hemolysin of *Staphylococcus aureus*. J Biol Chem 272:24858–24863

Vaz WLC, Nicksch A, Jahnig F (1978) Electrostatic interactions at charged lipid-membranes—measurement of surface pH with fluorescent lipoid pHindicators. Eur J Biochem 83:299–305

Vecsey-Semjen B, Mollby R, Gisou F, vander Goot FG (1996) Partial C-terminal unfolding is required for channel formation by staphylococcal alpha-toxin. J Biol Chem 271:8655–8660

Vecsey-Semjen B, Lesieur C, Mollby R, vander Goot FG (1997) Conformational changes due to membrane binding and channel formation by staphylococcal alpha-toxin. J Biol Chem 272: 5709–5717

Walker B, Bayley H (1995) Key residues for membrane-binding, oligomerization, and pore-forming activity of staphylococcal alpha-hemolysin identified by cysteine scanning mutagenesis and targeted chemical modification. J Biol Chem 270:23065–23071

Walker B, Krishnasastry M, Zorn L, Kasianowicz J, Bayley H (1992) Functional expression of the alpha-hemolysin of *Staphylococcus aureus* in intact *Escherichia coli* and in cell lysates—deletion of 5 C-terminal amino-acids selectively impairs hemolytic-activity. J Biol Chemistry 267:10902–10909

Winiski AP, Eisenberg M, Langner M, McLaughlin S (1988) Fluorescent probes of electrostatic potential 1 nm from the membrane surface. Biochemistry 27:386–392